

Grain boundary character modification employing thermo-mechanical processing in type 304L stainless steel

S K Pradhan* and S Mandal

Department of Metallurgical and Materials Engineering,
Indian Institute of Technology, Kharagpur-721302, W.B, India

*E-mail: sumanta14julymet@gmail.com

Abstract. Grain boundary engineering (GBE) approach has been employed to modify the boundaries character of a type 304L stainless steel through thermo-mechanical processing (TMP) route, which combined a low level of cold deformation (5, 10 and 15 %) followed by annealing at 1173K and 1273K for 1hour. Employing Electron Back Scatter Diffraction based Orientation Imaging Microscopy, the fraction and distribution of low Σ CSL boundaries ($\Sigma \leq 29$) and its effect on random high-angle grain boundaries connectivity and triple junction distribution of as-received (AR) and GBE specimens were evaluated. It was possible to increase the fraction of low Σ CSL boundaries up to 75% following GBE treatment (as compared to 50% in AR specimen). The GBE specimens also contained maximum number of percolation resistant triple junctions which could render better resistance against percolation related phenomena.

Keywords: Grain boundary engineering; Thermo-Mechanical processing; Triple junction distribution; CSL boundaries Introduction

1. Introduction

Grain boundary engineering (GBE) is relatively a new concept on the basis of controlling the grain boundary character distribution (GBCD) in many alloy systems [1-4]. Generally low Σ coincidence site lattice (CSL) boundaries ($\Sigma \leq \Sigma 29$) exhibit some special behaviors in comparison to random high angle grain boundaries (HAGBs). Proportion of $\Sigma 3$ and its variant like $\Sigma 9$ and $\Sigma 27$ boundaries have been enhanced in the past to modify boundary related properties in low stacking fault energy FCC materials [5,6] like resistance against solute segregation [7], inter-granular corrosion (IGC) [8-10], stress corrosion cracking (SCC) [11], creep and fatigue [12,13]. The main objective of GBE is to enhance the materials properties by increasing the fraction of low CSL grain boundaries and to disrupt the connectivity of random HAGBs.

Thermo-mechanical processing (TMP) is the most effective approach to achieve GBE microstructure in complex alloys. The combination of deformation amount as well as annealing temperature and time needs



to be optimized for a material under investigation [14]. Type 304L stainless steel is widely used because of its better mechanical properties along with excellent corrosion resistance over a large temperature range. However, at a particular temperature range (sensitization temperature), the material is susceptible to inter-granular corrosion (IGC) and inter-granular stress corrosion cracking (IGSCC). Population, distribution and connectivity along with the nature of the boundaries are mainly responsible for inter-granular corrosion. The objective of this study is to understand the evolution of special boundaries and its effect on the connectivity of random HAGBs as well as triple junction distribution (TJD) in as-received (AR) and GBE-treated specimens of type 304L stainless steel.

2. Experimental Details

The material used in this study is type 304L stainless steel and its chemical compositions (in wt %) is given in Table 1. AR specimens were subjected to three different thickness reductions (viz. 5, 10 and 15pct) at room temperature by laboratory cold rolling mill. Deformed specimens were subsequently annealed at two different temperatures (1173 K and 1273 K) for 1 hour followed by water quenching (WQ). The TMP treatment employed in this investigation has been summarized in Table 2.

Table 1: Chemical composition (in wt %) of 304L stainless steel

C	Cr	Ni	P	S
0.0147	17.7	13.7	0.0032	0.0028

Table 2: Thermo-mechanical processing conditions adopted in this work

Specimen name	Processing conditions
AR	As-Received
R5-1173K	5% cold rolled + 1173 K for 1 h + WQ
R5-1273K	5% cold rolled + 1273 K for 1 h + WQ
R10-1173K	10% cold rolled + 1173 K for 1 h + WQ
R10-1273K	10% cold rolled + 1273 K for 1 h + WQ
R15-1173K	15% cold rolled + 1173 K for 1 h + WQ
R15-1273K	15% cold rolled + 1273 K for 1 h + WQ

The AR and GBE-treated specimens were polished up to 0.25 μm grit diamond paste using the standard metallographic polishing procedure. Specimens were further polished with colloidal silica (0.04 μm) suspension to ensure removal of any residual surface deformation. Electron Back Scatter Diffraction

(EBSD) based Orientation Imaging Microscopy (OIM) scans were performed on all the processed specimens to determine the GBCD in the materials using a TSL-OIM system attached to Zeiss Merlin scanning electron microscope operating at 20 kV. A step size of 0.5 μm was used for the orientation imaging. Misorientations above 2° were considered as grain boundaries. To identify CSL boundaries, Brandon's criterion [15] is used. Random HAGBs are defined as those with misorientation $\theta > 15^\circ$ and which are not low Σ ($\Sigma \leq 29$) CSL boundaries. The grain size was measured using linear intercept method (average of horizontal and vertical intercept lengths) and a misorientation of 5° was used for determining the grain size.

3. Results & Discussion

3.1. Characterization of GBs

The grain boundary plus image quality map of the AR and GBE-treated specimen (R5-1273K) is shown in Fig. 1(a) and Fig. 1(b), respectively. In addition to increase in the fraction of $\Sigma 3$, the frequency of $\Sigma 9$ and $\Sigma 27$ has been increased significantly in GBE-treated specimen. In AR specimen, most of the $\Sigma 3$ boundaries lie within the grains and are not part of the grain boundary network (see Fig. 1a). However, the random HAGBs have been substantially replaced by a large number of twin and its variants (i.e. $\Sigma 9$ and $\Sigma 27$) in GBE-treated specimen with moderate increase in grain size. It is to be noted that average grain size (considering twin as grain boundary) of AR and R5-1273K specimen is 14 μm and 21 μm , respectively.

Formation of annealing twins is mostly favored in low stacking fault energy FCC metals or alloys like 304L stainless steel [5]. Twin boundaries may form in two ways such as by "growth accident" mechanism during recrystallization [16] and/or by the movement of grain boundaries during GBE type TMP [5,6,9,17]. It is observed (Fig. 1a) that the $\Sigma 3$ boundaries in AR specimen are straight as well as parallel and terminate within a single grain. Further, the fractions of $\Sigma 9$ and $\Sigma 27$ boundaries are very small which indicates that the interaction between $\Sigma 3$ is insignificant. Therefore, it is logical to assume that the annealing twins in AR specimen have been formed by "growth accident" mechanism [9,16,17]. The morphology of $\Sigma 3$ boundaries in GBE-treated specimen is different – these boundaries are part of grain boundary network (see Fig. 1b). In addition to $\Sigma 3$ boundaries, the fraction of other annealing twin variants (i.e. $\Sigma 9$ and $\Sigma 27$) is also significantly high in GBE specimen. Maximum numbers of triple junctions are formed via interaction between twin and its variants and this is only possible by " $\Sigma 3$ regeneration mechanism" initiated through strain induced grain boundary migration (SIBM) [12,14,17]. Hence, it may be inferred that the GBE microstructures have been evolved via grain boundary migration initiated through TMP [6,9,17].

Figure 2 shows the 2D grain boundary networks excluding low Σ ($\Sigma \leq 29$) CSL boundaries in order to qualitatively assess the degree of connectivity of random HAGBs. In AR specimen, random high angle grain boundary length density ($\text{BLD}_{\text{RHAGB}}$ length of RHAGBs per unit area) value is very high (0.062 μm^{-1}) and random HAGBs networks are interconnected (see Fig. 2a). In contrast to this, the $\text{BLD}_{\text{RHAGB}}$ (0.021 μm^{-1}) has been decreased as well as connectivity of random HAGBs has been substantially

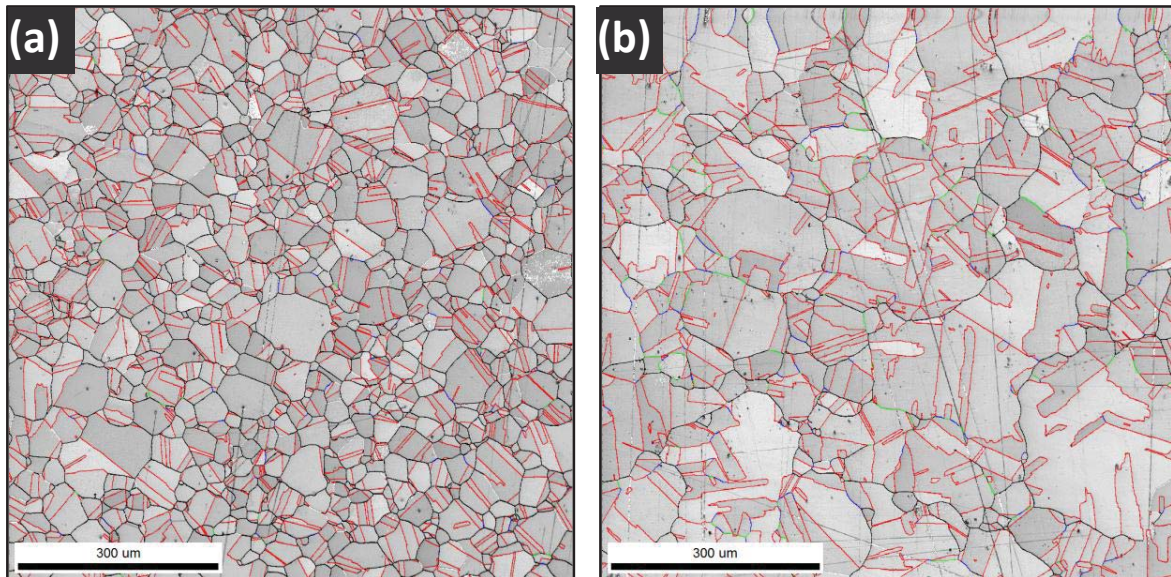


Figure 1: Grain boundary plus image quality (IQ) map of the (a) as-received and (b) GBE treated (R5-1273K) specimen. In orientation maps GBs are colour-coded as follows: $\Sigma 3$ —red; $\Sigma 9$ —blue; $\Sigma 27$ —green; random HAGBs—black)

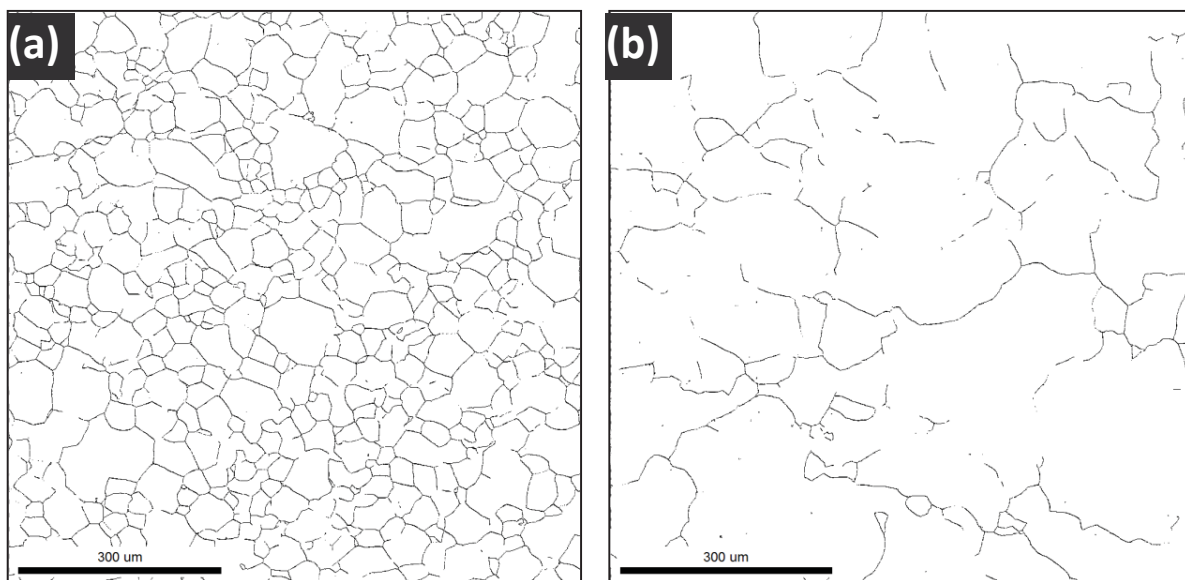


Figure 2: Grain boundary map showing the connectivity of random HAGBs in (a) as-received and (b) GBE treated (R5-1273K) specimen.

disrupted in GBE treated specimen (see Fig. 2b). It is important to note here that one has to increase the fraction of special boundaries and also need to break the random HAGBs networks in order to achieve

GBE microstructure [18]. This is due to the fact that boundary related properties of materials strongly depend on the type, density and connectivity of boundaries [7,8,10-13,19].

3.2 GBCD and Triple junction

Figure 3 shows the GBCD in AR and GBE-treated specimens. It could be observed the fraction of low Σ CSL boundaries have been significantly increased in all the specimens following GBE treatment. Especially in the R5-1273K specimen, low Σ CSL boundaries have increased to 75% from 50% in AR condition whereas $\Sigma 3$ boundaries have increased to 65% from the 44%. The

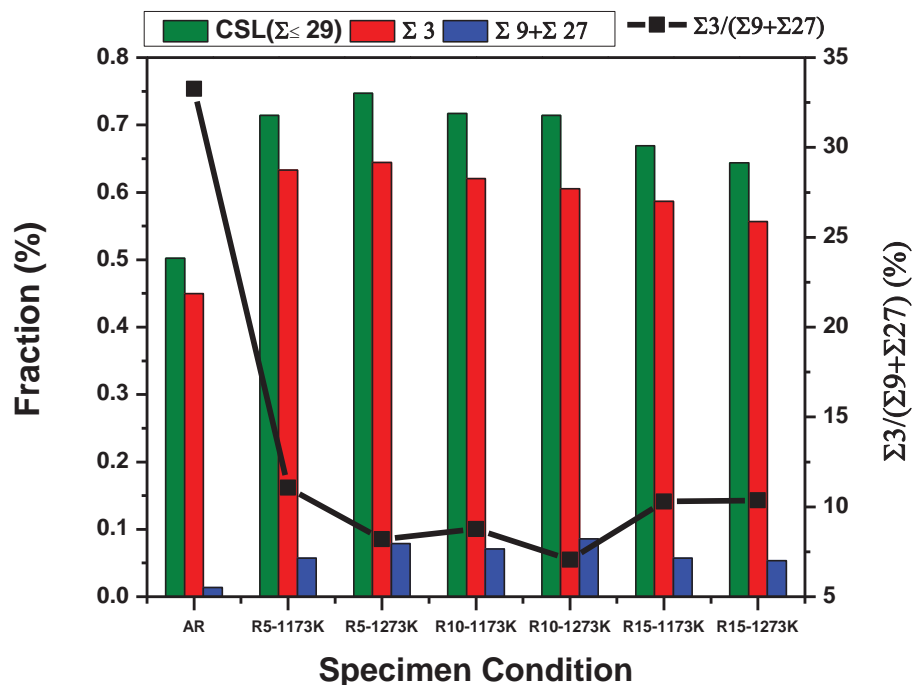


Figure 3: GBCD shown as fraction of CSL ($\leq \Sigma 29$), $\Sigma 3$ and ($\Sigma 9 + \Sigma 27$) in AR and GBE-treated specimens. The ratio of $\Sigma 3 / (\Sigma 9 + \Sigma 27)$ is also shown to assess random HAGBs connectivity

Increase in $\Sigma 3$ following deformation and annealing emphasize the role of strain induced grain boundary migration necessary for the creation of special boundaries [14,17,19]. However, percentage of low Σ CSL boundaries marginally decreases towards higher level of cold deformation (see Fig. 3). It is also seen from Fig. 3 that the proportions of second and third order twins (i.e. $\Sigma 9 + \Sigma 27$) are more than 5% in the GBE-treated specimens (with 5pct and 10pct pre-strain and annealed at 1273K). These higher order twin boundaries are preferable because they have the ability to generate large number of $\Sigma 3$ boundaries on the basis of ‘‘ $\Sigma 3$ regeneration mechanism’’ which states that $\Sigma 3^{n+1} + \Sigma 3^n = \Sigma 3$ occurs more frequently at triple junctions than $\Sigma 3^{n+1} + \Sigma 3^n = \Sigma 3^{n+2}$ [3,5,17]. Further, these higher order $\Sigma 3$ boundaries take part in reconfiguration of the existing grain boundary networks. Hence, the ratio of $\Sigma 3$ to ($\Sigma 9 + \Sigma 27$) parameter

provides better indication of the fragmentation of random HAGBs networks [14,17]. This ratio found to decrease from 34 in AR specimen to 7 and 4 in R5-1273K and R10-1273K specimen, respectively (Fig. 3). This correlate well with OIM generated random HAGBs connectivity map of R5-1273K specimen (see Fig. 2b) clearly indicating substantial disruption in random HAGBs connectivity in GBE treated specimen.

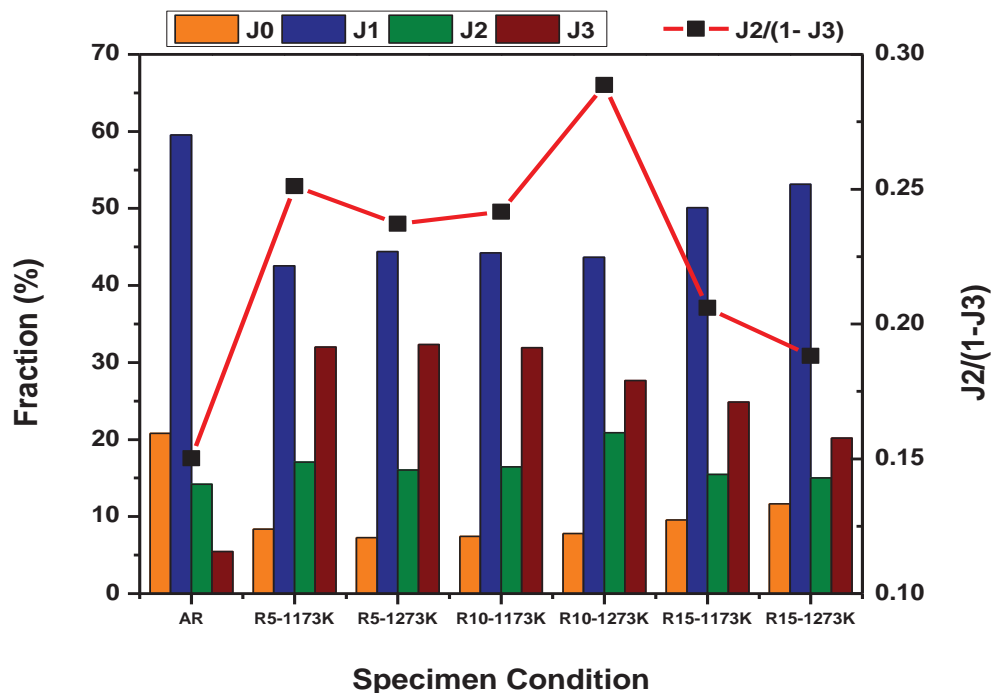


Figure 4: Triple junction distribution in AR and GBE-treated specimens

Triple junction (J_n) (where J_n indicates the fraction of triple junctions which have n low Σ CSL boundaries, $n = 0, 1, 2,$ or 3) distribution for AR and GBE specimens is shown in Fig. 4. It is to be noted here that J_3 -triple junctions are fully resistant against percolation related phenomena [6]. In this investigation, approximately 34% J_3 -triple junctions are achieved in R5-1173K, R5-1273K and R10-1173K specimens in contrast to 5% in AR condition. Therefore, it could be easily inferred that the substitution of random HAGBs through formation and interaction of special boundaries increase the percolation-resistant triple junction. According to Schuh et al, $J_2/(1-J_3)$ could be used as an important parameter to measure the probability of crack arrest for inter-granular crack propagation as well as resistance to percolation related phenomena [20]. It could be observed that $J_2/(1-J_3)$ is maximum for the specimen R10-1273K owing to the large population of J_2 -triple junction with intermediate number of J_3 -triple junction (see Fig. 4). This value is also high in R5-1273K specimen. Hence, it could be envisaged here that both the R5-1273K and R10-1273K specimens may exhibit better resistance against percolation-related phenomena.

4. Conclusions

Thermo-mechanical processing involving small strain (5% and 10% cold rolling) and high-temperature annealing has led to GBE microstructure in a type 304L stainless steel. The maximum fraction of low Σ CSL boundaries (75% as compared 50% in AR specimen) has been obtained with 5% pre-strain following annealing at 1273K for 1 hour. The GBE specimens have also found to contain maximum number of percolation resistant J_2 and J_3 -triple junctions. Hence the GBE specimens could exhibit better resistance against percolation related phenomena.

References

- [1] Watanabe T 1984 *Res. Mech.* **11** 47
- [2] Watanabe T 1988 *Mat. Forum* **11** 284
- [3] Randle V and Owen G 2006 *Acta Mater.* **54** 1777
- [4] Randle V 2006 *Scripta Mater.* **54** 1011
- [5] Randle V 1999 *Acta mater.* **47** 4187
- [6] Randle V 2004 *Acta Mater.* **52** 4067
- [7] Kobayashi S, Tsurekawa S, Watanabe T and Palumbo G 2010 *Scripta Mater.* **62** 294
- [8] Xia S, Li H, Liu T G and Zhou B X 2011 *J. Nucl. Mater.* **416** 303
- [9] Mandal S, Bhaduri A K and Sarma VS 2012 *Mat. S. Forum* **702** 714
- [10] Hu C, Xia S, Li H, Liu T G, Zhou B X, Chen W and Wang N 2011 *Corr Sc.* **53** 1880
- [11] Telang A, Gill A S, Tammana D, Wen X, Kumar M, Teyseyre S, Mannava S R, Qian D and Vasudevan V K 2015 *Mat. Sci. and Eng. A* **648** 280
- [12] Randle V 1996 *The Role of the Coincidence Site Lattice in Grain Boundary Engineering*, The Institute of Materials, London.
- [13] Kobayashi S, Kamata A and Watanabe T 2015 *Acta Mater.* **91** 70
- [14] Mandal S, Sivaprasad P V, Raj B and Sarma V S 2008 *Metal. Mater. Trans. A* **39** 3298
- [15] Brandon D G 1966 *Acta Metall.* **14** 1479
- [16] Gleiter H 1969 *Acta Mater.* **17** 1421
- [17] Mandal S, Bhaduri A K and Sarma V S 2011 *J. Mat. Sci.* **46** 275
- [18] Lee S L and Richards N L 2005 *Mat. Sci. and Eng. A* **405** 74
- [19] Shimada M, Kokawa H, Wang Z J and Karibe I 2002 *Acta Mater.* **50** 2331
- [20] Schuh C A, Kumar M and King W 2003 *Acta Mater.* **51** 687